THE JOURNAL OF PHYSICAL CHEMISTRY A

Article

pubs.acs.org/JPCA

Photodissociation Dynamics of Gaseous $CpCo(CO)_2$ and Ligand Exchange Reactions of $CpCoH_2$ with C_3H_4, C_3H_6, and NH_3

Melania Oana, Yumiko Nakatsuka, Daniel R. Albert, and H. Floyd Davis*

Department of Chemistry and Chemical Biology, Cornell University, Ithaca, New York 14853, United States

Supporting Information

ABSTRACT: The photodissociation dynamics of $CpCo(CO)_2$ was studied in a molecular beam using photofragment translational energy spectroscopy with 157 nm photoionization detection of the metallic products. At 532 and 355 nm excitation, the dominant one-photon channel involved loss of a single CO ligand producing CpCoCO. The product angular distributions were isotropic, and a large fraction of excess energy appeared as product vibrational excitation. Production of CpCO + 2CO resulted from two-photon absorption processes. The two-photon dissociation of mixtures containing $CpCo(CO)_2$ and H_2 at the orifice of a pulsed nozzle was used to produce a novel 16-electron unsaturated species, $CpCoH_2$. Transition metal ligand exchange reactions, $CpCoH_2 + L \rightarrow CpCoL + H_2$ (L = propyne, propene, or ammonia), were studied under single-collision conditions for the first time. In all cases, ligand exchange occurred via 18-electron association complexes with lifetimes comparable to their rotational periods. Although ligand exchange reactions were not detected from $CpCoH_2$ collisions with methane or propane (L = CH_4 or C_3H_8), a molecular beam containing $CpCoCH_4$ was produced by photolysis of mixtures containing $CpCo(CO)_2$ and CH_4.

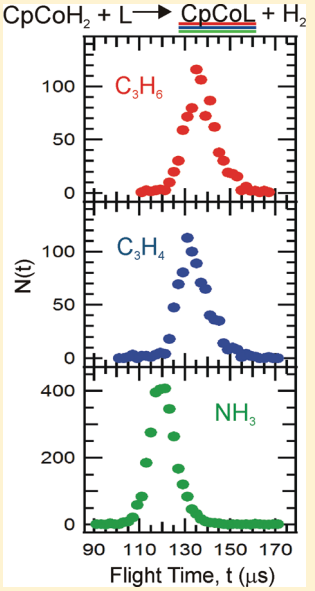

INTRODUCTION

One of the holy grails of transition metal chemistry is to develop complexes able to activate the C−H and C−C bonds of hydrocarbon molecules.[1] In solution, a number of unsaturated 16-electron transition metal complexes readily undergo ligand exchange reactions with hydrocarbons by formation of donor−acceptor addition complexes, or in certain cases, by C−H or C−C insertion.[2] One of the most studied family of systems is CpMCO or Cp*MCO where M = Co, Rh, or Ir, Cp = η^5-C_5H_5, and Cp* = η^5-$C_5(CH_3)_5$. This family of 16-electron species are readily produced by photolysis of the stable $CpM(CO)_2$ or $Cp^*M(CO)_2$ precursors.[3,4] To date, the photochemistry of $CpM(CO)_2$ and $Cp^*M(CO)_2$, as well as the reactivity of the photogenerated unsaturated products was studied primarily by transient infrared absorption spectroscopy in solution or in high pressure gas cells.[5−9] It is well-known that the photolytically produced Rh and Ir complexes readily insert into C−H bonds,[3−6] whereas CpCoCO is relatively unreactive with alkane and noble gas solvents. However, CpCoCO readily adds to $CpCo(CO)_2$ and to two-electron donors such as ethylene.[7−9] Theoretical calculations by Siegbahn suggested that the relatively inert behavior of CpCoCO toward alkanes is due to its ground triplet state electronic configuration. A large potential energy barrier prevents access to the reactive excited singlet state surface.[10] Such barriers do not exist for the heavier Rh and Ir complexes, which have been calculated to have ground singlet state electronic configurations.[10] An alternative hypothesis, proposed by Carreón-Macedo and Harvey, is that the lack of reactivity of CpCoCO is due to the thermoneutral nature of the addition reaction, leading to small equilibrium constants for production of the insertion complexes.[11]

The photodissociation dynamics of gaseous transition metal carbonyls have been the subject of numerous experimental studies. Although most work has concentrated on the first row transition metal compounds $Fe(CO)_5$,[12−14] $Ni(CO)_4$,[15] and $Cr(CO)_6$,[16] the behavior of some second and third row analogues, $Mo(CO)_6$[17] and $W(CO)_6$,[18] has also been studied.[19−21] Early condensed-phase experiments (in liquid solutions and in low-temperature inert gas matrixes) reported the loss of only one CO molecule upon photolysis, followed by relaxation of the metallic photofragment through collisions and recombination with the solvent.[20−22] However, photodissociation of gas phase samples at low pressures or under molecular beam collisionless conditions led to stepwise loss of several CO molecules.[12−18,20] After the first photolytic CO elimination, the $M(CO)_{n-1}$ photofragment underwent secondary spontaneous CO dissociation. In many cases, further spontaneous decomposition was possible, depending on the energetics.[23−26]

Received: February 26, 2012
Revised: May 3, 2012
Published: May 7, 2012

dx.doi.org/10.1021/jp3018919 | J. Phys. Chem. A 2012, 116, 5039−5044

For example, photodissociation of $Fe(CO)_5$ at 248 nm generated substantial amounts of $Fe(CO)_3$, while at 193 nm, the major product was found to be $Fe(CO)_2$.[12−14] The CO vibrational and rotational distributions were in agreement with a microcanonical statistical model in which the energy available to each photofragment after CO elimination is randomized prior to the next CO dissociation event.[13] To date, all studies of $CpCo(CO)_2$ photochemistry have involved samples at high gas pressure or in solution.[3−9] We sought to gain insight into the production of CpCoCO and other possible products by studying the photodissociation dynamics of $CpCo(CO)_2$ using photofragment translational energy spectroscopy. Under these conditions, the primary photochemistry can be elucidated in the absence of secondary stabilizing collisions.

It was clear from our studies that we could produce intense photolytic beams of CpCoCO. There have been a number of previous studies of C−H bond activation involving unsaturated transition metal atom complexes in the gas phase.[5,7,19] Much detail has also been learned about C−H activation involving bare transition metal atoms in fast flow reactors and in crossed molecular beams.[27−31] However, there have been no reports of studies of reactions involving unsaturated ligated complexes carried out under single-collision conditions in crossed molecular beams. We sought to study the insertion chemistry of CpCoCO with hydrocarbon molecules under single-collision conditions. Significant activation energy for C−H bond insertion was anticipated due to the triplet ground state character of CpCoCO.[10,11] To surmount such barriers, CpCoCO was seeded in the lightest carrier gas, H_2, in order to increase the reactant velocity and resulting collision energy. Although we easily observed bimolecular chemistry, the dominant reactive species produced in beams containing H_2 was found to be $CpCoH_2$, rather than CpCoCO. In this article, we describe our experimental results, which represent the first crossed molecular beam studies of transition metal ligand exchange reactions.

EXPERIMENTAL SECTION

All experiments were carried out utilizing the Cornell rotatable sources crossed molecular beams machine, described in detail previously.[32] In the photodissociation experiments, a pulsed supersonic molecular beam of $CpCo(CO)_2$ (Strem Chemicals) was generated by passing He carrier gas through a room temperature bubbler containing $CpCo(CO)_2$ and expanding the mixture through the 1 mm orifice of a piezoelectric pulsed valve. The $CpCo(CO)_2$ beam (v = 1750 m/s; speed ratio = 21) was collimated by a series of two skimmers, 1 mm and 2 mm diameter respectively, before entering the main chamber and crossing the photodissociation laser. The second (532 nm) or third (355 nm) harmonic of a Nd:YAG laser (Continuum Surelite) were used for photodissociation. The photodissociation laser was gently focused into the interaction region to a ∼3 mm spot size. Typical pulse energies used were ∼10 mJ/pulse. For power dependence studies, the laser power was varied using a half waveplate and a pile of plates polarizer.

In the ligand exchange reactions, a molecular beam of $CpCoH_2$ was generated by expanding $CpCo(CO)_2$ in a carrier gas (pure H_2 or 8% Ar in H_2) and photolyzing $CpCo(CO)_2$ at the output of the 1 mm diameter pulsed valve orifice with the third harmonic (355 nm) of a Nd:YAG laser focused to a 5 by 2 mm spot. In the photolysis volume at high laser powers, a two-photon process occurs that forms CpCo + 2 CO. Since the photolysis occurs in the collisional region of the supersonic expansion, CpCo photolysis products can subsequently collide with H_2 to form $CpCoH_2$ by collisional 3-body stabilization. The $CpCoH_2$ beam was collimated by the same two skimmers used in the photodissociation experiments and passed into the main chamber, where it was intersected at a 90° crossing angle by a second pulsed beam (20% C_3H_6 in H_2, 20% C_3H_4 in H_2, or 5% NH_3 in H_2). The use of two skimmers as defining elements for the $CpCoH_2$ beam reduces the angular divergence of the beam to 1.25°. The second pulsed beam was generated by supersonic expansion of a gas mixture through the 1 mm orifice of a second piezoelectric pulsed valve and collimated by a 1 mm diameter skimmer before entering the main chamber.

After the cobalt-containing beam was crossed by either a laser pulse or a molecular beam, products traveled 24.1 cm into the ionization region of a triply differentially pumped quadrupole mass spectrometer detector, where they were ionized by the 7.9 eV output of an F_2 excimer laser (GAM Laser EX100HF), mass filtered, and detected with a multiplier/conversion dynode detector operating in pulse counting mode. Time-of-flight (TOF) spectra were generated at a given laboratory angle by scanning the 7.9 eV laser relative to the photodissociation laser. Laboratory angular distributions were generated by integrating the TOF distribution for each laboratory angle. The secondary beams (20% propene, C_3H_6, in H_2; 20% propyne, C_3H_4, in H_2; or 5% ammonia, NH_3, in H_2) were analyzed in separate experiments by using a chopper wheel to select a portion of the molecular beam and sending the molecular beam directly into the detector, where the species were detected using an electron impact ionizer (100 eV) and the quadrupole mass spectrometer. Beam velocities, speed ratios, and corresponding collision energies (E_{coll}) for each crossed molecular beams experiment are shown in Table 1.

Table 1. Collision Energies and Beam Parameters for Ligand Exchange Reactions

E_{coll} (kJ/mol)	$CpCoH_2$ carrier gas	beam velocity (m/s)	speed ratio	secondary gas mixture	beam velocity (m/s)	speed ratio
126 ± 8	H_2	2410	17	20% C_3H_4 in H_2	1600	17
67 ± 5	8% Ar in H_2	1500	17	20% C_3H_4 in H_2	1440	14
113 ± 7	H_2	2400	17	20%C_3H_6 in H_2	1240	14
62 ± 4	8% Ar in H_2	1510	15			
80 ± 5	H_2	2360	17	5% NH_3 in H_2	2210	15
56 ± 3	8% Ar in H_2	1530	14			

The data was fit using the forward-convolution technique, assuming a separable center-of-mass (CM) translational energy release, $P(E)$, and CM angular distribution, $T(\Theta)$. The fitting program took as inputs a trial $P(E)$ and $T(\Theta)$ along with measured beam velocities, speed ratios, angular divergences, detector aperture sizes, etc. and calculated TOF spectra and laboratory angular distributions.[33] The calculated TOF spectra and laboratory angular distributions were then compared with their experimental counterparts, and the $P(E)$ and $T(\Theta)$ distributions were iteratively adjusted to optimize the agreement between the calculated and experimental distributions.

dx.doi.org/10.1021/jp3018919 | J. Phys. Chem. A 2012, 116, 5039−5044

RESULTS AND DISCUSSION

Photodissociation of $CpCo(CO)_2$. We studied the photodissociation of $CpCo(CO)_2$ at 355 and 532 nm. The products of photodissociation were found to be CpCoCO (m/e = 152) + CO and CpCo (m/e = 124) + 2CO. The TOF spectra and angular distribution, recorded at m/e = 152, for 355 nm photodissociation producing CpCoCO + CO are shown in Figure 1. Each TOF spectrum corresponds to ~15 000 laser shots (10 min of data collection time). At angles near the $CpCo(CO)_2$ beam (3° and 5°), some background exists from fragmentation of $CpCo(CO)_2$ to CpCoCO caused by the 7.9 eV radiation in the ionization region. The parent fragmentation background was subtracted by performing experiments with the photolysis laser blocked from entering the main chamber. The signal recorded at m/e = 152 for CpCoCO + CO was found to have linear dependence on the photodissociation laser pulse energy, whereas the signal recorded at m/e = 124 for CpCo + 2 CO was found to have quadratic dependence on the photodissociation laser pulse energy (Figure 2). Therefore, the loss of two CO molecules involves a two photon process.

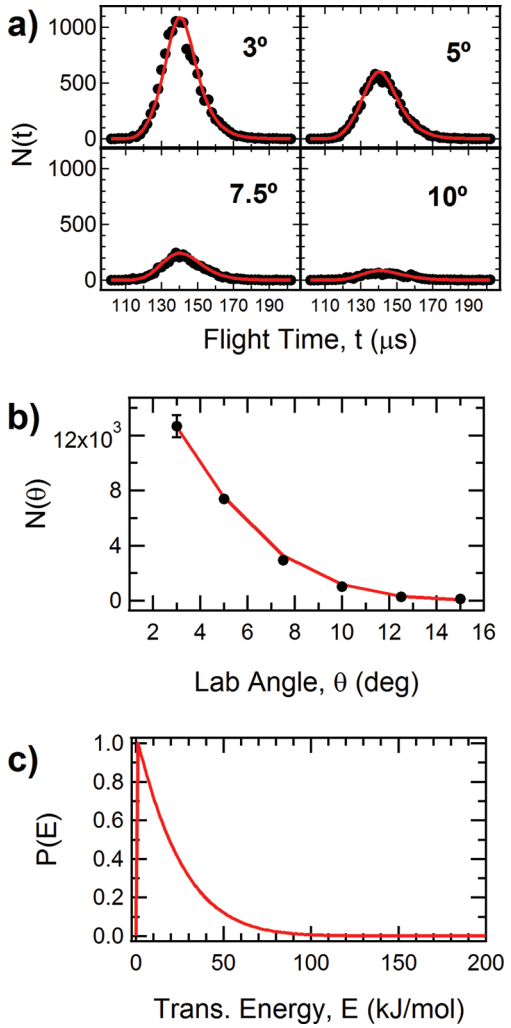

Figure 1. (a) Time-of-flight (TOF) spectra of CpCoCO (m/e = 152) (solid circles) recorded at indicated laboratory angles for 355 nm photodissociation. Solid line fits were generated using the $P(E)$ shown below. (b) Laboratory angular distribution of CpCoCO (solid circles) for 355 nm photodissociation and the fit (solid line) generated using the $P(E)$ shown below. (c) CM translational energy distribution used to fit the CpCoCO experimental data for 355 nm photodissociation.

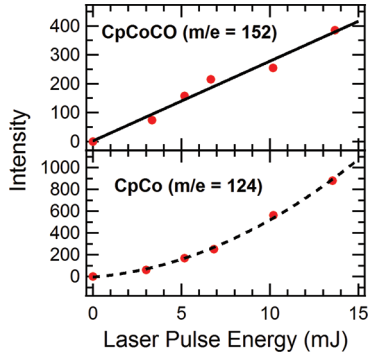

Figure 2. Integrated TOF signal from 355 nm photodissociation at 12° as a function of laser power for $CpCoCO^+$, m/e = 152, and $CpCo^+$, m/e = 124; solid line shows linear least-squares fit to m/e = 152 data; dotted line shows quadratic least-squares fit to m/e = 124 data.

The data for CpCoCO + CO were fit using a $P(E)$ peaking at zero translational energy release, with the $P(E)$ tail extending up to approximately 85 kJ/mol (Figure 1), and an isotropic product angular distribution. The $P(E)$ used to fit the 532 nm photodissociation, available as Supporting Information, also peaks at zero translational energy release but extends to only 30 kJ/mol. A $P(E)$ peaking at zero translational energy release (large internal excitation) is consistent with previous studies of metal carbonyls, where energy was distributed throughout the entire complex before dissociation.[13]

Baer and co-workers[34] determined D_0[CpCo(CO)−CO] = 184 kJ/mol using photoelectron spectroscopy. In theoretical calculations, Siegbahn[10] and Harvey[11] calculated similar values of 222 and 225 kJ/mol, respectively. The maximum kinetic energy release from the 532 nm photodissociation is consistent with the D_0[CpCo(CO)−CO] measurement of Baer and co-workers[34] and inconsistent with the larger calculated values of Siegbahn[10] and Harvey.[11] The first Co−CO bond in $CpCo(CO)_2$ is relatively strong for a transition metal carbonyl, which typically have bond strengths in the 95−230 kJ/mol range.[23−26] The maximum translational energy release represents approximately 50% of the total energy available at both 355 and 532 nm photodissociation after subtracting the binding energy of the first CO (Table 2).[34] Although there have been no experimental measurements of D_0(CpCo−CO), Baer and co-workers found the dissociation energy of CpCoCO → Cp + Co + CO to be 385 kJ/mol.[34] After subtracting the CpCoCO−CO bond dissociation energy, the excess energy above the dissociation threshold is only 152 kJ/mol for 355 nm photodissociation. Considerable vibrational excitation is expected in the CpCoCO and CO products. Our finding that the dominant channel involves loss of a single CO at 355 nm is consistent with these thermodynamic considerations.

Table 2. Energy Available for Photodisoociation Experiments

photolysis wavelength (nm)	photon energy (kJ/mol)	energy available after CO loss (kJ/mol)
532	225	41
355	337	152

dx.doi.org/10.1021/jp3018919 | J. Phys. Chem. A 2012, 116, 5039−5044

Ligand Exchange Reactions of $CpCoH_2$. Two photon dissociation of $CpCo(CO)_2$ at 355 nm in the presence of H_2 was used to produce the $CpCoH_2$ beam. Reactive scattering data for the reaction, $CpCoH_2 + L \rightarrow CpCoL + H_2$ (L = C_3H_4, C_3H_6, or NH_3), were recorded at two different collision energies for each of the molecular reactants L. The collision energies used in this study are summarized in Table 1. The TOF spectra for the reaction at E_{coll} = 67 kJ/mol with C_3H_4, recorded at m/e = 164, are shown in Figure 3. These TOF spectra were integrated to generate the laboratory angular distributions shown in Figure 4. The CM distributions used to calculate the fits to the data along with the corresponding error limits are shown in Figure 4. From the error limits in the $P(E)$ distributions, shown as the green line in Figure 4, the $P(E)$ is peaking away from zero, near 40 kJ/mol. Because of the relatively large uncertainty limits on the maximum translational energy release, it is not possible to derive much insight into the thermodynamics of the reaction. The large uncertainty is due to the kinematics of the system. Because of conservation of linear momentum, the recoil velocity of the detected $CpCoC_3H_4$ (m = 164 u) in the CM frame of reference is 82 times smaller than that of the H_2 counterfragment (m = 2 u). Consequently, the laboratory velocity of the $CpCoC_3H_4$ is primarily determined by the CM velocity of the system, rather than the recoil velocity of the $CpCoC_3H_4$. This can be visualized via the Newton diagram shown in Figure 5; where the two Newton circles correspond to the maximum and most probable $CpCoC_3H_4$ recoil velocities. Even with the large speed ratios and well-collimated beams in the present work, the error limits of the $P(E)$ distributions for H_2 elimination remain large. In future experiments, the use of D_2 rather than H_2 should improve our

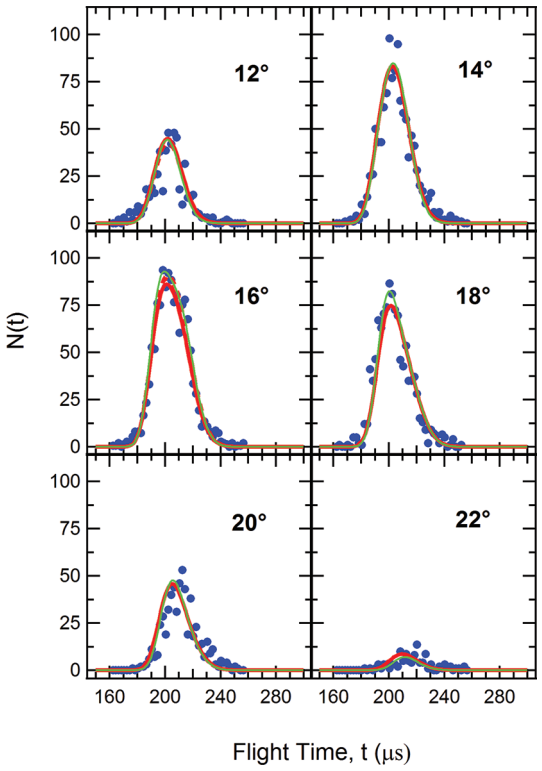

Figure 3. Measured TOF spectra for indicated laboratory angles for $CpCoC_3H_4^+$ (m/e = 164) from the 67 kJ/mol collision energy reaction. Solid circles represent experimental data points; red lines were generated using the optimized CM distributions shown in Figure 4; green lines were generated using the optimized $T(\Theta)$ and the $P(E)$ shown in green in Figure 4.

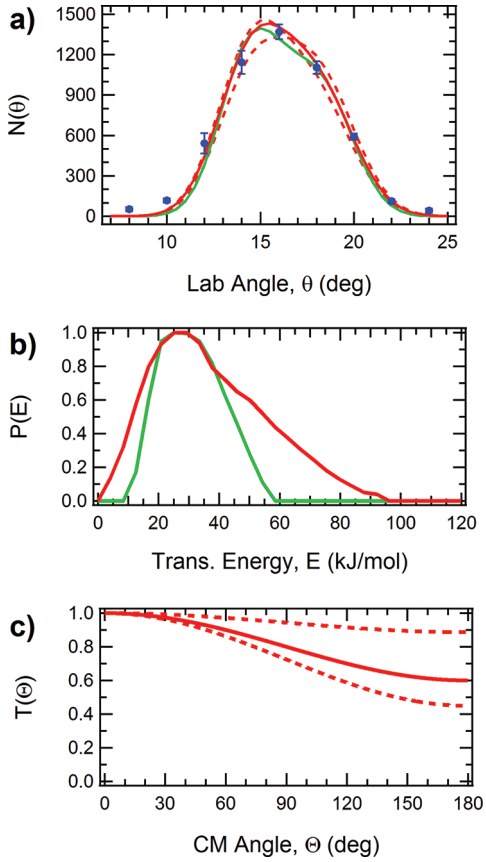

Figure 4. (a) Laboratory angular distributions for $CpCoC_3H_4$ (m/e = 164) from the 67 kJ/mol reaction. Solid circles are experimental data with 1σ error bars; solid red line represents optimized fit using CM distributions shown below; dotted lines represent error limits for the CM angular distribution using the optimized $P(E)$ shown below; solid green line represents fit generated using the optimized $T(\Theta)$ and green $P(E)$ shown below. (b) CM translational energy release, $P(E)$; solid red line represents optimized $P(E)$; solid green line represents error limit for $P(E)$ using optimized $T(\Theta)$. (c) CM angular distribution, $T(\Theta)$; solid red line represents optimized $T(\Theta)$; dotted red lines represent error limits for $T(\Theta)$ using optimized $P(E)$.

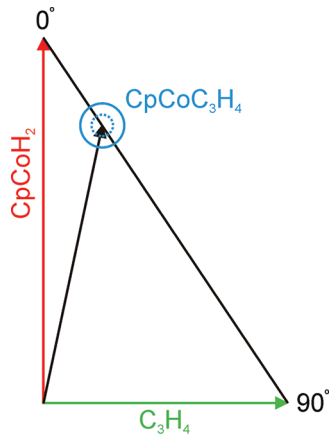

Figure 5. Newton diagram for the 126 kJ/mol $CpCoH_2$ + C_3H_4 reactive scattering; the solid circle represents the maximum $CpCoC_3H_4$ recoil velocity; the dotted circle represents the most probable $CpCoC_3H_4$ recoil velocity. Laboratory angles are indicated.

dx.doi.org/10.1021/jp3018919 | J. Phys. Chem. A 2012, 116, 5039−5044

ability to gain thermodynamic insight into these ligand exchange reactions.

The TOF spectra, laboratory angular distribution, and CM distributions for $CpCoH_2 + C_3H_4 \rightarrow CpCoC_3H_4 + H_2$ at E_{coll} = 126 kJ/mol are shown in Figures 6 and 7. The CM angular

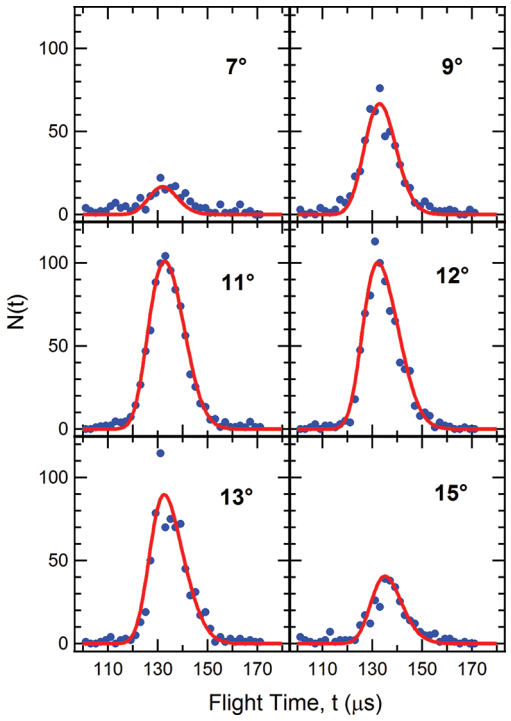

Figure 6. Measured TOF spectra of $CpCoC_3H_4^+$ (m/e = 164) for indicated laboratory angles from the 126 kJ/mol collision energy reaction. Solid circles represent experimental data points; red lines were generated using the optimized CM distributions shown in Figure 7.

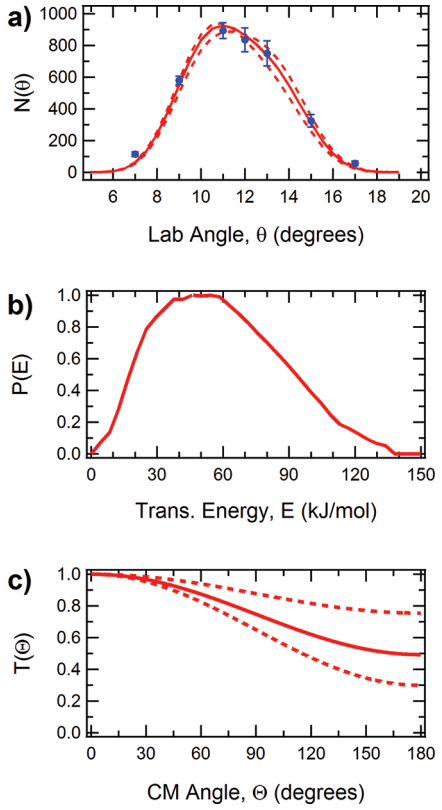

Figure 7. (a) Laboratory angular distributions for $CpCoC_3H_4^+$ (m/e = 164) from the 126 kJ/mol reaction. Solid circles are experimental data with 1σ error bars; solid red line represents optimized fit using CM distributions shown below; dotted lines represent error limits for the CM angular distribution using the optimized $P(E)$ shown below. (b) CM translational energy release, $P(E)$; solid red line represents optimized $P(E)$. (c) CM angular distribution, $T(\Theta)$; solid red line represents optimized $T(\Theta)$; dotted red lines represent error limits for $T(\Theta)$ using optimized $P(E)$.

distributions at both collision energies are characterized by asymmetric distributions peaking in the forward direction. The error limits for each fit are denoted by the dotted lines in Figures 4 and 7. An asymmetric distribution can be interpreted as an osculating complex with intermediates having lifetimes that are comparable to a rotational period[35] or as the reaction proceeding through multiple mechanisms. One plausible scenario in the present case would involve the combination of a forward−backward symmetric distribution, corresponding to reactions involving complexes that are long-lived relative to their rotational periods superimposed on a forward scattered distribution, involving a direct reaction mechanism.[36] As the collision energy is increased, the CM angular distribution was found to become slightly more forward scattered, implying either decreased average lifetimes for the reaction intermediates or an increased contribution from the direct forward scattering mechanism.[35,36] The CM distributions used to fit the data from the reactions with C_3H_6 and NH_3 are similar to those used for the reaction with C_3H_4 and are shown in the Supporting Information. For all ligand exchange reactions studied, the $P(E)$ peaked away from zero at modest translational energy release, 30−40 kJ/mol, and the $T(\Theta)$ is slightly asymmetric, again peaking in the forward direction. The $CpCoH_2 + L \rightarrow CpCoL + H_2$ reactions are all characterized by C_3H_4, C_3H_6, or NH_3 associatively adding to the 16-electron $CpCoH_2$ species forming an 18-electron $CpCoH_2L$ complex. These complexes then decay, with lifetimes comparable to their rotational periods, forming $CpCoL + H_2$ with a modest barrier for elimination or decay back to reactants forming $CpCoH_2 + L$.

No exchange reactions were observed for $CpCoCO + L \rightarrow CpCoL + CO$ or $CpCo(CO)_2 + L \rightarrow CpCoCOL + CO$ (L = C_3H_4, C_3H_6, or NH_3). The CpCoCO beam intensities were ~2 times weaker than $CpCoH_2$ beam intensities, whereas $CpCo(CO)_2$ beam intensities were at least 5 times more intense than $CpCoH_2$ beam intensities. The detection sensitivities for these channels are estimated to be about an order of magnitude smaller than for the corresponding $CpCoH_2$ reactions. However, if the cross-sections for exchange reactions involving CpCoCO or $CpCo(CO)_2$ were at least 20% of those for the $CpCoH_2$ reactions, because of the high signal-to-noise ratio using 157 nm photoionization detection, we would expect to have easily observed the CpCoCO or $CpCo(CO)_2$ reactions. As previously discussed by others, the small reactivity toward alkanes[7−9] is likely due to the existence of potential energy barriers for C−H insertion owing to the triplet ground state of CpCoCO.[10]

No ligand exchange reactions were observed for collisions of $CpCoH_2$ with methane or propane. However, we were able to make beams containing $CpCoCH_4$ complexes, in a manner analogous to that for production of $CpCoH_2$, i.e., by seeding $CpCo(CO)_2$ in a carrier gas containing CH_4. The absence of

dx.doi.org/10.1021/jp3018919 | J. Phys. Chem. A 2012, 116, 5039−5044

ligand exchange reactions of $CpCoH_2$ with alkanes suggests the existence of potential energy barriers for addition. While the ground state multiplicity of $CpCoH_2$ is not known, by analogy with CpCoCO, it may be a triplet.[10,11] As in the case for CpCoCO, a high-spin ground state electronic state configuration for $CpCoH_2$ could lead to appreciable potential energy barriers for the addition to form $CpCoH_2(CH_3)(H)$. In contrast, because the addition of $CpCoH_2$ to alkenes and to NH_3 can proceed *without* insertion, these association reactions are likely to be facile even if $CpCoH_2$ has a triplet ground state. Electronic structure calculations would provide considerable insight into this observed behavior.

CONCLUSIONS

The photodissociation of $CpCo(CO)_2$ producing CpCoCO + CO was studied at 355 and 532 nm. This process was characterized by an isotropic product angular distribution and low translational energy release, i.e., large internal excitation, at both photolysis wavelengths. Loss of a second CO was also observed but determined to occur primarily via a two-photon process. This two-photon process was exploited to form a molecular beam of $CpCoH_2$, which was found to undergo ligand exchange reactions under crossed molecular beam conditions, forming CpCoL + H_2, where L = C_3H_4, C_3H_6, or NH_3. These reactions involve reaction intermediates whose lifetimes are similar to a rotational period; however, little thermodynamic information could be derived from the present experiments due to the large uncertainty in the $P(E)$ arising from the unfavorable kinematics of the system. Ligand exchange reactions were not observed for L= CH_4 or C_3H_8. One possible explanation for the inability for $CpCoH_2$ to insert into the C−H bonds of alkanes is the existence of sizable potential energy barriers for insertion, possibly due to a triplet ground state for $CpCoH_2$, analogous to that for CpCoCO.[10,11]

In future experiments, we plan to study ligand exchange reactions of $CpCoCH_4$ or $CpCoD_2$ with small molecules (L). For both of these systems, because of the heavier recoil partners (CH_4 or D_2) accompanying production of CpCoL, the improved kinematics should considerably enhance our ability to gain experimental insight into the thermodynamics of these prototype transition metal ligand exchange reactions.

ASSOCIATED CONTENT

Supporting Information

TOF data and fits from the 532 nm photodissociation of $CpCo(CO)_2$ and from the ligand exchange reactions of $CpCoH_2$ with propene and ammonia. This material is available free of charge via the Internet at http://pubs.acs.org.

AUTHOR INFORMATION

Corresponding Author

*E-mail: hfd1@cornell.edu.

Notes

The authors declare no competing financial interest.

ACKNOWLEDGMENTS

We would like to thank Professor Roald Hoffmann and Professor Barry Carpenter for valuable discussions. This research was supported by the National Science Foundation under Grant CHE-0809622.

REFERENCES

(1) Labinger, J. A.; Bercaw, J. E. *Nature* **2002**, *417*, 507−514.
(2) Richens, D. T. *Chem. Rev.* **2005**, *105*, 1961−2002.
(3) Lees, A. J. *J. Organomet. Chem.* **1998**, *554*, 1−11.
(4) Hoyano, J. K.; Graham, W. A. G. *J. Am. Chem. Soc.* **1982**, *104*, 3723−3725.
(5) Wasserman, E. P.; Moore, C. B.; Bergman, R. G. *Science* **1992**, *255*, 315−318.
(6) Bromberg, S. E.; Lian, T.; Bergman, R. G.; Harris, C. B. *J. Am. Chem. Soc.* **1996**, *118*, 2069−2072.
(7) Wasserman, E. P.; Bergman, R. G.; Moore, C. B. *J. Am. Chem. Soc.* **1988**, *110*, 6076−6084.
(8) Dougherty, T. P.; Heilweil, E. J. *J. Chem. Phys.* **1994**, *100*, 4006−4009.
(9) Bengali, A. A.; Bergman, R. G.; Moore, C. B. *J. Am. Chem. Soc.* **1995**, *117*, 3879−3880.
(10) Siegbahn, P. E. M. *J. Am. Chem. Soc.* **1996**, *118*, 1487−1496.
(11) Carreón-Macedo, J.-L.; Harvey, J. N. *J. Am. Chem. Soc.* **2004**, *126*, 5789−5797.
(12) Ray, U.; Brandow, S. L.; Bandukwalla, G.; Venkataraman, B. K.; Zhang, Z.; Vernon, M. *J. Chem. Phys.* **1988**, *89*, 4092−4101.
(13) Waller, I. M.; Hepburn, J. W. *J. Chem. Phys.* **1988**, *88*, 6658−6669.
(14) Venkataraman, B. K.; Bandukwalla, G.; Zhang, Z.; Vernon, M. *J. Chem. Phys.* **1989**, *90*, 5510−5526.
(15) Schlenker, F. J.; Bouchard, F.; Waller, I. M.; Hepburn, J. W. *J. Chem. Phys.* **1990**, 7110−7118.
(16) Tyndall, G. W.; Jackson, R. L. *J. Chem. Phys.* **1989**, *91*, 2881−2891.
(17) Buntin, S. A.; Cavanagh, R. R.; Richter, L. J.; King, D. S. *J. Chem. Phys.* **1991**, *94*, 7937−7950.
(18) Venkataraman, B. K.; Hou, H.; Zhang, Z.; Chen, S.; Bandukwalla, G.; Vernon, M. *J. Chem. Phys.* **1990**, *92*, 5338−5362.
(19) Rayner, D. M.; Ishikawa, Y.; Brown, C. E.; Hackett, P. A. *Laser Chem. Organomet.* **1993**, 96−105.
(20) Weitz, E. *J. Phys. Chem.* **1994**, *98*, 11256−11264.
(21) Long, C. Photophysics of CO Loss from Simple Metal Carbonyl Complexes. In *Photophysics of Organometallics*, 1st ed.; Lees, A. J., Ed.; Springer-Verlag: Berlin, Germany, 2010; Vol. *29*, pp 37−72.
(22) Wrighton, M. *Chem. Rev.* **1974**, *74*, 401−430.
(23) Engelking, P. C.; Lineberger, W. C. *J. Am. Chem. Soc.* **1979**, *101*, 5569−5573.
(24) Stevens, A. E.; Feigerle, C. S.; W. Lineberger, C. *J. Am. Chem. Soc.* **1982**, *104*, 5026−5031.
(25) Lewis, K. E.; Golden, D. M.; Smith, G. P. *J. Am. Chem. Soc.* **1984**, *106*, 3905−3912.
(26) Sunderlin, L. S.; Wang, D.; Squires, R. R. *J. Am. Chem. Soc.* **1992**, *114*, 2788−2796.
(27) Wen, Y.; Porembski, M.; Ferrett, T. A.; Weisshaar, J. C. *J. Phys. Chem. A* **1998**, *102*, 8362−8368.
(28) Pederson, D. B.; Zgierski, M. Z.; Anderson, S.; Rayner, D. M.; Simard, B.; Li, S.; Yang, D.-S. *J. Phys. Chem. A* **2001**, *105*, 11462−11469.
(29) Campbell, M. L. *J. Phys. Chem. A* **1998**, *102*, 892−896.
(30) Senba, K.; Matsui, R.; Honma, K. *J. Phys. Chem.* **1995**, *99*, 13992−13999.
(31) Hinrichs, R. Z.; Schroden, J. J.; Davis, H. F. *J. Phys. Chem. A* **2008**, *112*, 3010−3019.
(32) Willis, P. A.; Stauffer, H. U.; Hinrichs, R. Z.; Davis, H. F. *Rev. Sci. Instrum.* **1999**, *70*, 2606−2614.
(33) Willis, P. A.; Stauffer, H. U.; Hinrichs, R. Z.; Davis, H. F. *J. Phys. Chem. A* **1999**, *103*, 3706−3720.
(34) Sztáray, B.; Szepes, L.; Baer, T. *J. Phys. Chem. A* **2003**, *107*, 9486−9490.
(35) Fisk, G. A.; McDonald, J. D.; Herschbach, D. R. *Faraday Discuss. Chem. Soc.* **1967**, *44*, 228−229.
(36) Estillore, A. D.; Visger, L. M.; Suits, A. G. *J. Chem. Phys.* **2010**, *133*, 074306.